Interaction Notes

Note 591

August 16, 2004

Example of the Use of the BLT Equation for EM Field Propagation and Coupling Calculations

F.M. Tesche
J. Keen
C. M. Butler

Holcombe Dept. of Electrical and Computer Engineering
College of Engineering & Science
337 Fluor Daniel Building
Box 340915
Clemson, SC 29634-0915

Abstract

This note provides a numerical verification of the extended BLT equation for a transmission line structure located in the vicinity of a perfect ground plane. The line is excited by a nearby infinitesimal current element, and as a consequence, it is illuminated by a spherical wave having a 1/r fall-off of the field intensity. Using suitable Green's functions for the ground plane effects, an extended BLT equation for the transmission line voltages and the E-field at observation locations is formulated. Solutions are obtained both numerically and symbolically. One key issue in this analysis is including both the common mode (antenna) and differential mode (transmission line) contributions to the scattered field from the line. At the conclusion of this note, there are several suggestions of future work that could be performed in this area.

Work conducted under the provisions of AFOSR MURI Grant F49620-01-1-0436

Contents

Figures

Example of the Use of the BLT Equation for EM Field Propagation and Coupling Calculations

1. Introduction

The original BLT (Baum-Liu-Tesche) equation was developed for determining the voltage and current responses at the nodes of a general multiconductor transmission line network [1]. As noted in this and other references [2], the solutions for these responses using the BLT equation are *approximate*, in that they involve the assumptions of transmission line theory to describe the behavior of the electromagnetic waves being propagated along the branches (or "tubes") of the network. Recently, an extension of the BLT equation concept was proposed to include the effects of EM field propagation in space (along trajectories that can be thought of as being an imaginary field propagation "tube") [3]. In this development, the possibility of non-plane wave propagation was suggested, and the coupling of these fields to the lines was taken into account. Moreover, the re-radiation of EM fields from the transmission line currents is provided. With these effects included, an extended BLT equation was formulated, with observables being a combination of both transmission line voltage and E-field responses.

In the present note, the use of the extended BLT equation developed in ref.[3] is illustrated with a numerical example. A simple geometry is postulated involving a 2-wire transmission line, which is a structure that is appropriate for a conventional BLT analysis. However, this line is excited by a transient current element located near the line, and consequently, the excitation of the line is by a spherical wave. Moreover, the line is located next to a conducting ground plane, and this affects both the incident field exciting the line and the re-radiation of the line. A distant observation point is also defined in this problem, and the solution for the E-field at this location is also included in the BLT formulation.

All of these features are included in the extended BLT equation, which permits an analysis in the frequency domain. Included in this analysis is not only the transmission line response, but the common mode (or antenna mode) response of the transmission line structure, which has an effect on the scattered field. As will be noted in what follows, however, these scattered fields from the antenna are small compared with the primary fields emitted from the source.

It is important to point out at the onset of this analysis, that while spherical waves are used to represent the EM fields propagating to and from source and field observation points, these fields are assumed to be locally plane waves at the transmission line structure.

2. Problem Description and Geometry

The problem under discussion here involves a simple two-wire transmission line illuminated by an electric and/or a magnetic source, as shown in Figure 1. This line/source configuration is similar to that examined in ref.[3], with the exception that now an infinite, perfectly conducting ground plane is added to the structure.

As in the problem discussed in [3], the goal of the present analysis is to develop an *extended* BLT equation for computing the two load voltages on the transmission line, as well as the E-fields at a distant observation point and at the transmission line.

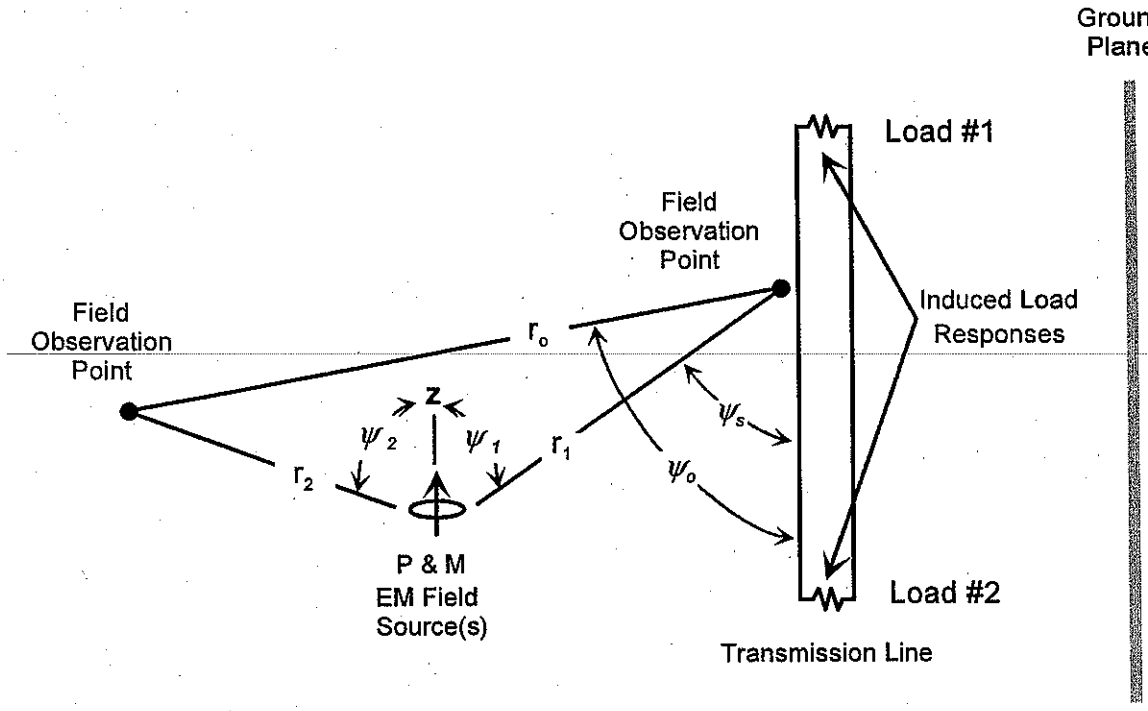

Figure 1. Geometry of a simple elementary source exciting a transmission line.

In performing this analysis, the following assumptions are made:

1. The distances between the source, transmission line, ground plane and any observation points are assumed to be large compared with the wavelength, so that far-field expressions for radiated or scattered fields can be used.

2. The transmission line cross-section is assumed to be electrically small, so that the induced differential mode response can be represented by transmission line theory. The transmission line length can be comparable or larger than the wavelength.

3. The currents on the two-wire line are portioned into differential mode (transmission line) and common mode (antenna) components. The common mode response has no effect on the transmission line load responses, as it is zero at the ends of the line. However, it does affect the response of the EM field at distant observation points. The differential mode current response is calculated using conventional transmission line theory, and the common mode response is calculated using an approximate transmission line-like solution.

4. The transmission line equations for the propagating voltage and current waves on the line in the presence of the ground plane are assumed to be identical to those of an isolated line. The excitation field for this line, however, is modified by the ground plane. This is equivalent to saying that the transmission is loosely coupled to its ground plane image.

The $\vec{P}$ and $\vec{M}$ sources shown in Figure 1 radiate an EM field towards the transmission line (in a direction defined by the angle ψ_1) and towards the observation point (in a direction defined by the angle ψ_2). Due to the anisotropic nature of the radiation from general sources, the amplitudes of the EM fields in these directions will be different. Also shown in Figure 1 is the angle of incidence ψ_s of a field *incident* on the transmission line, and a scattering angle, ψ_o, which corresponds to an angle at which the *radiated* E-field from the transmission line is observed.

The specific example of the two-wire line considered in this note is shown in Figure 2. The transmission line consists of two parallel conductors, each of radius a and length L, and separated by a distance d. This line is terminated by two impedance elements, ZL_1 and ZL_2, and the induced voltages across these loads are the observation quantities. This line is located parallel to an infinite ground plane, at a distance h from the center of the line.

The excitation source for this problem is taken to be an infinitesimal source with current moment *Idl*. This source is parallel to both the transmission line and the ground plane (in the z-direction), and is located on the y-axis at a distance r_1 from the transmission line center. The field observation point is also located along the y-axis at a distance r_2 from the source, as shown in the figure. For this geometry the various angles discussed above are all equal: $\psi_1 = \psi_2 = \psi_o = \psi_s = \pi/2$.

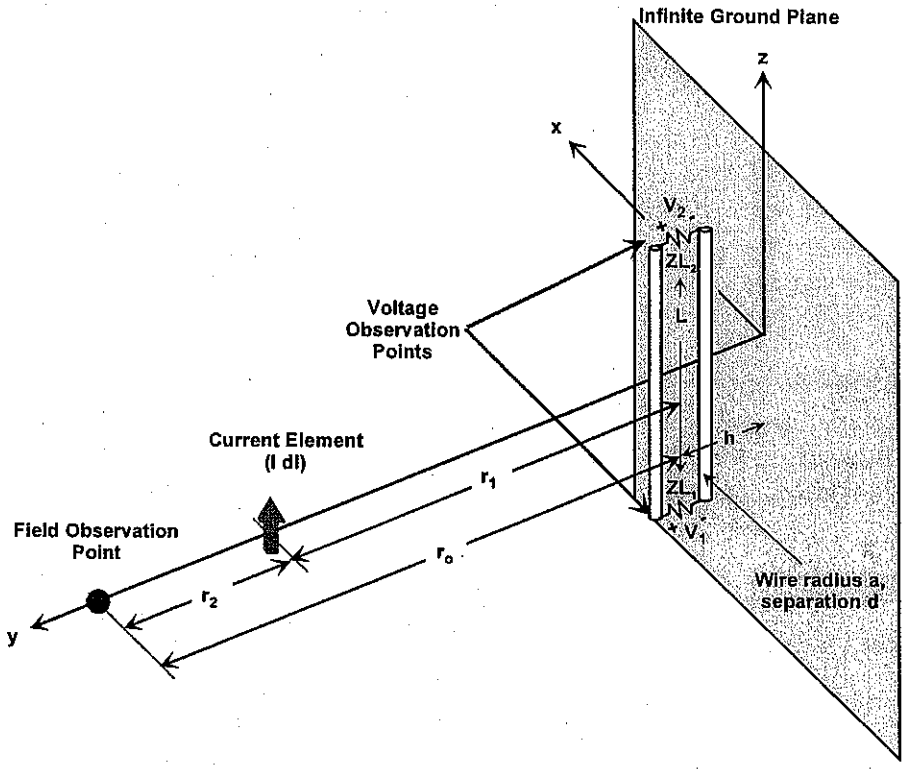

Figure 2. Specific example of the line geometry of a simple elementary source exciting a transmission line.

As discussed in ref.[3], the signal flow graph for the problem *without* the ground plane is the simple two tube, four node graph shown in Figure 3. With the ground plane present, the signal flow graph for the excited transmission line is the same, but the EM field coupling and propagation relationships on the tubes are formulated using modified Green's functions that take into account the presence of the conducting plate. Details of these Green's functions are provided in the next section.

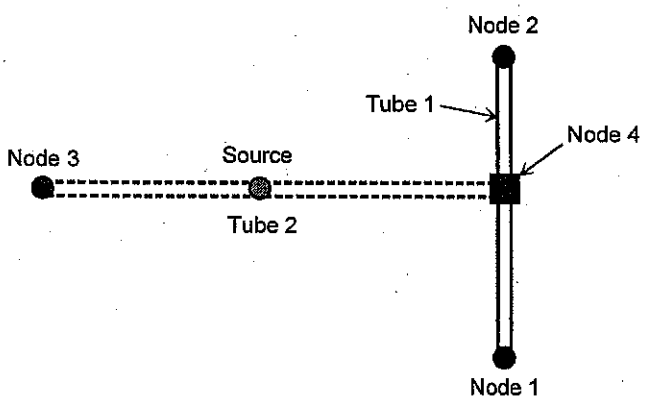

Figure 3. The signal flow graph for the EM interaction geometry of Figure 2.

3. The Extended BLT Equation

The derivation of the extended BLT equation for this problem begins by defining traveling wave components of positive and negative traveling voltage waves on the transmission line (tube 1), and similar positive and negative propagating E-field waves on the field propagation tube (tube 2). These traveling waves are determined at each of the nodes in the network, and are re-expressed as *incident* and *reflected* waves at the nodes. Figure 4 illustrates the incident and reflected voltages and E-fields on the signal flow graph.

The development of the extended BLT equation for this network involves combining both the tube propagation relationships and the node reflection relationships, as described in ref. [3]. However, in the present analysis with the ground plane, the effect of the ground plane on the field coupling and radiation of the transmission line must be taken into account.

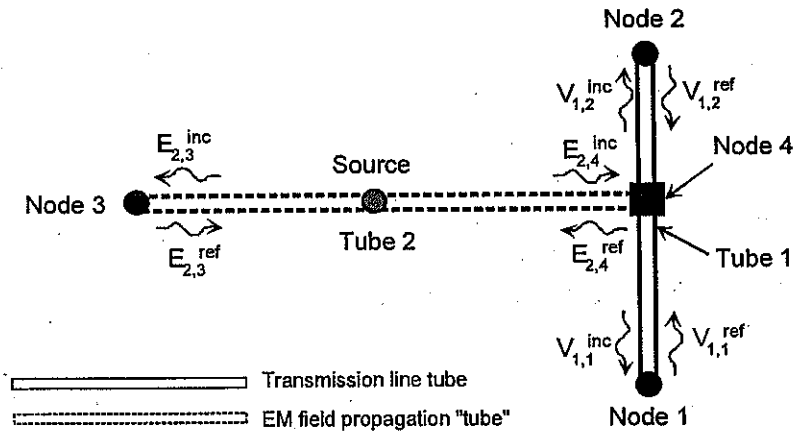

Figure 4. Definition of the incident and reflected voltages and E-fields on the signal flow graph.

3.1 Tube Propagation Relationships

3.1.1 Propagation on Tube 1 (the Transmission Line)

To begin with the development of the extended BLT equation, we first review the propagation relationships for the positive and negative traveling voltage waves on the transmission line. For the transmission line tube 1 *located in free space and excited by an incident plane wave*, ref. [3] has developed the following matrix equation relating the reflected and incident voltage waves at nodes 1 and 2:

$$\begin{bmatrix} V_{1,1}^{ref} \\ V_{1,2}^{ref} \end{bmatrix} = \begin{bmatrix} 0 & e^{\gamma L} \\ e^{\gamma L} & 0 \end{bmatrix} \cdot \begin{bmatrix} V_{1,1}^{inc} \\ V_{1,2}^{inc} \end{bmatrix} - \begin{bmatrix} F_1(\psi_s) E_{2,4}^{inc} \\ F_2(\psi_s) E_{2,4}^{inc} \end{bmatrix}. \tag{1}$$

As shown in Figure 5, the excitation of this line is provided by an incident EM field with the E-field in the plane of the transmission line and an angle of incidence ψ_S. This incident field induces charge and current everywhere on the line, and the specific observation quantities of interest are the load currents and voltages, as noted in the figure.

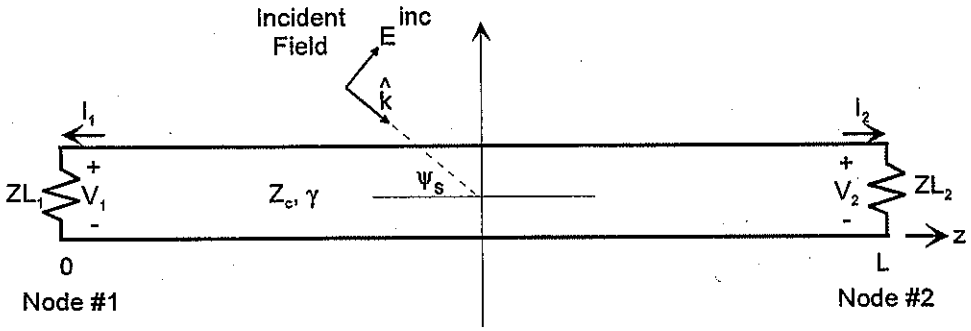

Figure 5. Field excitation of a two-wire transmission line.

For this lossless transmission line with wire radius a and separation d, the characteristic impedance of the line is

$$Z_c = \sqrt{(j\omega L')/(j\omega C')} = 120 \ln\left(\frac{d}{a}\right) \quad \Omega \qquad (2)$$

and simple TEM transmission line theory provides the wave propagation constant γ as

$$\gamma = j\frac{\omega}{c} \qquad (3)$$

where ω is the angular frequency ($2\pi f$) and c is the speed of light = 3.0×10^8 m/s.

Note that Eq.(1) contains two terms. The first is a matrix relationship relating the propagation of the incident and reflected voltage waves on the line. The second is a vector term that describes the excitation of voltage waves by the incident E-field $E^{inc}_{2,4}$ at the "field coupling node" (node 4), as introduced in ref.[3]. This excitation is represented by the integral functions $F_1(\psi_s)$ and $F_2(\psi_s)$ developed in Appendix A of [3], multiplied by the incident field $E^{inc}_{2,4}$. These F functions depend on the local angle of incidence on the line ψ_S, and in the more general case, on the azimuthal incidence and polarization angles (see Eq.(7.40) of ref.[2]). For the special geometry of Figure 2, the incident field on the transmission line is broadside to the line, so that $\psi_S = \pi/2$.

From Appendix A, the general expressions for the field coupling terms to the transmission line $F_1(\psi_s)$ and $F_2(\psi_s)$ are given as

$$F_1(\psi_s) = \frac{d}{2}\left(e^{jkL(1-\cos\psi_s)} - 1\right)$$
$$F_2(\psi_s) = \frac{d}{2}e^{jkL}\left(e^{-jkL(1+\cos\psi_s)} - 1\right) \quad , \tag{4}$$

and for $\psi_S = \pi/2$ these terms simplify to

$$F_1 = \frac{d}{2}\left(e^{jkL} - 1\right)$$
$$F_2 = \frac{d}{2}\left(1 - e^{jkL}\right) = -F_1 \tag{5}$$

It is important to note from Eq.(4) that the excitation of the line, and hence the line response, are *even* functions of the angle of incidence ψ_s on the transmission line. Thus, for the excitations shown in Figure 6, the line responses I_1, I_2, V_1 and V_2 will be identical for the two different incident fields.

The effect of this symmetry in the excitation of the differential (transmission line) mode when the line is located next to a conducting ground plane is suggested in Figure 7. In this case, the reflected E-field from the ground plane has a reversal of direction to satisfy the boundary condition that the tangential component of E is zero on the ground plane. This results in the ground plane-reflected field, which arrives with a negative angle of incidence, affecting the line exactly like the incident field in Figure 6, but with a different time delay. As a result, *both the incident and ground-reflected field components induce differential mode responses on the transmission line that have the same sign*. In other words, the contributions from these E-field components to the differential mode are <u>additive</u>.

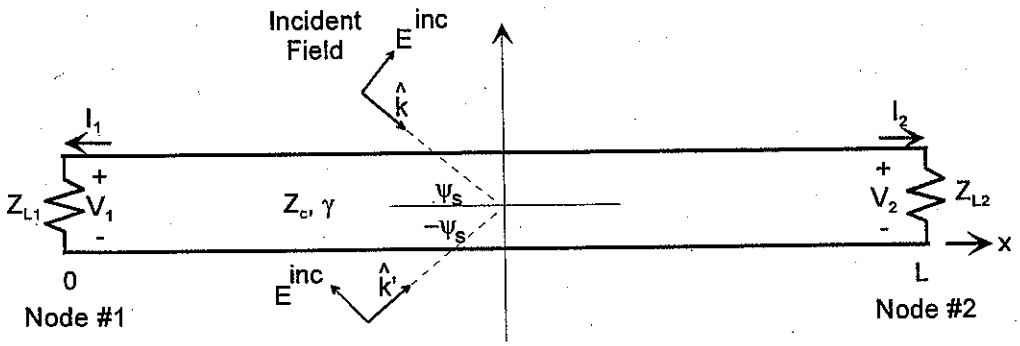

Figure 6. Line excitation for positive and negative angles of incidence, ψ_s.

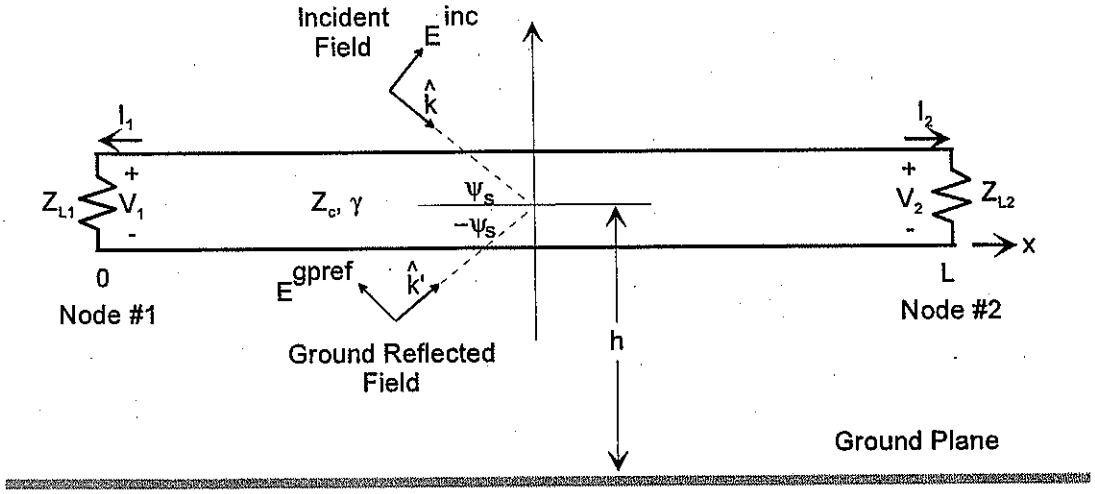

Figure 7. Transmission line located over a conducting ground plane and excited by an incident plane wave.

To extend Eq.(1) to the case of *plane wave* illumination of the transmission line located over the ground plane, we may superimpose the effects of the incident and ground plane-reflected fields. This provides the following matrix expression:

$$\begin{bmatrix} V_{1,1}^{ref} \\ V_{1,2}^{ref} \end{bmatrix} = \begin{bmatrix} 0 & e^{\gamma L} \\ e^{\gamma L} & 0 \end{bmatrix} \cdot \begin{bmatrix} V_{1,1}^{inc} \\ V_{1,2}^{inc} \end{bmatrix} - \begin{bmatrix} F_1(\psi_s)E^{inc} + F_1(-\psi_s)E^{gpref} \\ F_2(\psi_s)E^{inc} + F_2(-\psi_s)E^{gpref} \end{bmatrix} \tag{6}$$

In this last equation, E^{inc} denotes the incident E-field strength evaluated at the midpoint of the transmission line, and E^{gpref} represents the ground plane-reflected field strength at the same midpoint location.[1]

Assuming that the line height over the ground plane is h, using the excitation symmetry and taking the zero phase reference to be at the midpoint of the line, we find that Eq(6) for the incident and reflected line voltages at nodes 1 and 2 for a plane wave excitation becomes

$$\begin{bmatrix} V_{1,1}^{ref} \\ V_{1,2}^{ref} \end{bmatrix} = \begin{bmatrix} 0 & e^{\gamma L} \\ e^{\gamma L} & 0 \end{bmatrix} \cdot \begin{bmatrix} V_{1,1}^{inc} \\ V_{1,2}^{inc} \end{bmatrix} - \begin{bmatrix} F_1(\psi_s)E^{inc}(1+e^{-jk2h\sin(\psi_s)}) \\ F_2(\psi_s)E^{inc}(1+e^{-jk2h\sin(\psi_s)}) \end{bmatrix} \tag{7}$$

---

[1] Note that E^{inc} and E^{gpref} are the total fields, not the tangential fields along the line. (See Appendix A of [3] for details.)

where an *effective excitation term* $\mathcal{E}^{excit}$ has been defined as

$$\mathcal{E}^{excit} = E^{inc}(1+e^{-jk2h\sin(\psi_s)}). \tag{8}$$

Notice that the term $\mathcal{E}^{excit}$ is <u>not</u> the total E-field at the transmission line (which would be written as $E^{tot} = E^{inc}(1-e^{-jk2h\sin(\psi_s)})$), but rather, it is given by Eq.(8) with the plus sign for the exponential term. Since the assumed geometry of this problem involves only the z-components of the E-field (see Figure 2), the z-component of the E-field is identically zero on the ground plane (h = 0). The excitation term in (8), with the positive sign for the exponential term, becomes $2E^{inc}$. This is a field boundary condition more akin to that for the tangential magnetic field on a perfect conductor, than to that for the tangential E-field.

Using the notation $\mathcal{E}^{excit}$ for the effective line excitation, we write Eq.(7) as

$$\begin{bmatrix} V_{1,1}^{ref} \\ V_{1,2}^{ref} \end{bmatrix} = \begin{bmatrix} 0 & e^{\gamma L} \\ e^{\gamma L} & 0 \end{bmatrix} \cdot \begin{bmatrix} V_{1,1}^{inc} \\ V_{1,2}^{inc} \end{bmatrix} - \begin{bmatrix} F_1(\psi_s)\mathcal{E}^{excit} \\ F_2(\psi_s)\mathcal{E}^{excit} \end{bmatrix}. \tag{9}$$

Thus we see that the functional form of Eq.(1) may be used to describe the relationships between the incident and reflected voltage waves at nodes 1 and 2 of the transmission line with the E^{inc} terms in the excitation being modified by the effects of the ground plane, as represented by the excitation term $\mathcal{E}^{excit}$.

Of course, the expression for the excitation field in Eq.(8) is valid only for an incident plane wave. In the case of the infinitesimal current source excitation shown in Figure 1, a different form of this excitation function is required. Neglecting polarization effects and assuming far-field conditions hold, one can express the incident E-field on the transmission line by spherical waves from the current source *Idl* and possibly from a reflected field ($E_{2,3}^{ref}$) from the distant node 3, as

$$E^{inc} = \frac{e^{-jkr_o}}{r_o} a_3 E_{2,3}^{ref} + \frac{e^{-jkr_1}}{r_1} \mathcal{S}_1(\psi_1). \tag{10}$$

In this expression, the terms (e^{-jkr}/r) provide for the propagation of the spherical waves along tube 2. As discussed in ref.[3], the parameter a_3 represents a typical dimension of the scattering body at node 3 and is used as a normalizing constant for the E-fields to provide dimensions of voltage, and to provide a BLT equation for all variables having the same dimension.

The source term $\mathcal{S}_1(\psi_1)$ in Eq.(10) describes the amplitude of the radiation from the elementary current source in the direction given by the angle ψ_1, as shown in Figure 8. For this simple example of a *z*-directed current source, the *z*-component of the radiated E-field at the transmission line location is given as

$$E_z(\psi_1) = -\frac{j\omega\mu}{4\pi} Idl \sin^2(\psi_1) \frac{e^{-jkr_1}}{r_1}$$
$$\equiv \mathcal{S}_1(\psi_1) \frac{e^{-jkr_1}}{r_1} \tag{11}$$

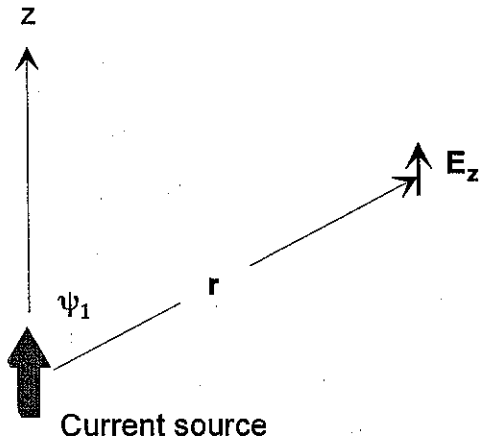

Figure 8. An elementary current source and the E_z field component at a distance r.

Equation (11) defines the source term $\mathcal{S}$ at an angle ψ_1 as $\mathcal{S}(\psi_1) = -j\omega\mu\, Idl \sin^2(\psi_1)$. For the example we are considering in Figure 2, the source angle is $\psi_1 = \psi_s = \pi/2$, so that the source term in Eq.(11) is

$$\mathcal{S}_1 = -\frac{j\omega\mu}{4\pi} Idl \tag{12}$$

With the spherical wave of Eq.(10) incident on the transmission line, another ground plane-reflected spherical wave also will be present, and both will contribute to the excitation of the line. From Eq.(10) and image theory, the following z-directed excitation E-field acting on the transmission line can be determined:

$$\mathcal{E}^{excit} = \left(\frac{e^{-jkr_o}}{r_o} + \frac{e^{-jk(r_o+2h)}}{r_o+2h}\right) a_3 E_{2,3}^{ref} + \left(\frac{e^{-jkr_1}}{r_1} + \frac{e^{-jk(r_1+2h)}}{r_1+2h}\right) \mathcal{S}_1$$
$$\equiv K_1(r_o) a_3 E_{2,3}^{ref} + K_1(r_1) \mathcal{S}_1 \tag{13}$$

Here the terms $K_1(r_o)$ and $K_1(r_1)$ amount to modified Green's functions representing the excitation functions for the transmission line in the presence of the ground plane. These are defined as

$$K_1(r) = \frac{e^{-jkr}}{r} + \frac{e^{-jk(r+2h)}}{r+2h}. \tag{14}$$

With this excitation term for the transmission line, the tube 1 matrix propagation relation of Eq.(9) for the spherical wave excitation becomes[2]

$$\begin{bmatrix} V_{1,1}^{ref} \\ V_{1,2}^{ref} \end{bmatrix} = \begin{bmatrix} 0 & e^{\gamma L} \\ e^{\gamma L} & 0 \end{bmatrix} \cdot \begin{bmatrix} V_{1,1}^{inc} \\ V_{1,2}^{inc} \end{bmatrix} - \begin{bmatrix} F_1 K_1(r_o) a_3 E_{2,3}^{ref} \\ F_2 K_1(r_o) a_3 E_{2,3}^{ref} \end{bmatrix} - \begin{bmatrix} F_1 K_1(r_1) \mathcal{S}_1 \\ F_2 K_1(r_1) \mathcal{S}_1 \end{bmatrix}. \tag{15}$$

3.1.2 Propagation on Tube 2 (the Field Propagation Path)

We now turn our attention to the behavior of the incident and reflected E-fields at nodes 3 and 4 on tube 2 – the field propagation path. Considering first the incident E-field at node 4, $E_{2,4}^{inc}$, we note that it consists of a direct term like Eq.(10) from the source and the reflected field at node 3, $E_{2,3}^{ref}$, together with the ground plane image contributions. This results in an equation similar to Eq.(13) for the excitation field of the transmission line, but with a *negative* sign for the image terms:

$$\begin{aligned} E_{2,4}^{inc} &= \left(\frac{e^{-jkr_o}}{r_o} - \frac{e^{-jk(r_o+2h)}}{r_o+2h} \right) a_3 E_{2,3}^{ref} + \left(\frac{e^{-jkr_1}}{r_1} - \frac{e^{-jk(r_1+2h)}}{r_1+2h} \right) \mathcal{S}_1 \\ &\equiv K_2(r_o) a_3 E_{2,3}^{ref} + K_2(r_1) \mathcal{S}_1 \end{aligned} \tag{16}$$

where the modified Green's function $K_2(r)$ is given as

$$K_2(r) = \left(\frac{e^{-jkr}}{r} - \frac{e^{-jk(r+2h)}}{(r+2h)} \right) \tag{17}$$

---

[2] Note that Eq.(15) is different from Eq.(9) for the isolated transmission line. The source term for Eq.(9) involves the just the incident E-field at the field coupling node (4), while in Eq.(15) the effective excitation source involves both the E-field reflected from node 3 *and* the radiated field from the current source. Both of these excitation fields are reflected in the ground plane (using the K_1 Green's functions), and then the original incident field components and the reflected fields are applied as excitation fields to the line, as indicated by Eq.(6). This is done because the excitation of the transmission line is not determined by the total incident E-field (e.g., the sum of the incident plus ground plane reflected field at node 4), but rather, the excitation depends on both the incident field strength *and* on the direction of incidence (see Figure 6). In this manner, the excitation of the line is constructed so that the signs of the incident and ground-reflected field components are correct.

Similarly, with the transmission line (tube 1) absent, the E-field propagation relationship for the incident E-field $E_{2,3}^{inc}$ at node 3 (the field observation point) is expressed using image theory as:

$$E_{2,3}^{inc} = \left(\frac{e^{-jkr_o}}{r_o} - \frac{e^{-j(kr_o+2h)}}{(r_o+2h)} \right) a_4 E_{2,4}^{ref} + \left(\frac{e^{-jkr_2}}{r_2} - \frac{e^{-jk(r_2+2r_1+2h)}}{r_2+2r_1+2h} \right) \mathcal{S}_2(\psi_2)$$

$$\equiv K_2(r_o) a_4 E_{2,4}^{ref} + K_3(r_2) \mathcal{S}_2(\psi_2) \qquad (18)$$

In this expression, a characteristic length of node 4 (a_4) is used for normalization of the field. Also, a third modified E-field Green's function $K_3(r)$ is introduced to account for the ground plane effects, as

$$K_3(r) = \left(\frac{e^{-jkr}}{r} - \frac{e^{-jk(r+2r_1+2h)}}{r+2r_1+2h} \right). \qquad (19)$$

The source term $\mathcal{S}_2(\psi_2)$ in Eq.(18) generally involves a different angle than does the source in Eq.(16), as noted from Figure 1. However, for our example of Figure 2, this angle is the same as ψ_1. so that $\mathcal{S}_2(\psi_2) = \mathcal{S}_1(\psi_1) = -\frac{j\omega\mu}{4\pi} Idl$.

If the transmission line is inserted into the problem space, then the transmission line mode currents flowing on the line also contribute to the incident E-field at node 3. As noted in Appendix B of ref.[3], the radiated E-field at a distance r_o and observation angle ψ_o from the transmission line currents flowing in the 2-wire line of Figure 9 can be expressed in terms of the incident voltage waves at each node of the transmission line of the line (nodes 1 and 2) as

$$E_\xi = \frac{jk}{2\pi} \frac{Z_o}{Z_c} \frac{e^{-jkr_o}}{r_o} \left(V_1^{inc} F_1(\psi_o) + V_2^{inc} F_2(\psi_o) \right), \qquad (20)$$

where Z_o is the free space wave impedance ($Z_0 \approx 377\ \Omega$), Z_c is the characteristic impedance of the transmission line ($Z_c = 120 \ln(d/a)\ \Omega$ for wire radius a and separation d), and $k = 2\pi f / c$. The field radiation terms F_1 and F_2 are the same as these derived for the reception case in Eq.(4), but evaluated for the observation angle ψ_o.

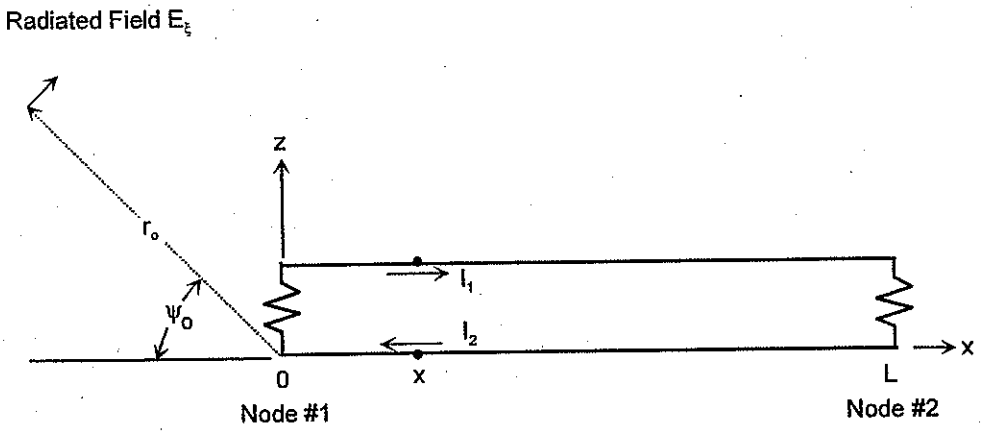

Figure 9. Illustration of a transmission line radiating an E_ξ-field component in a direction given by the angle ψ_o.

Equation (20) is not the complete expression for the radiation from the transmission line, however, as the ground plane effects have not yet been taken into account. Figure 10 shows the transmission line positioned near the ground plane and illustrates the fact that the wire currents of the transmission line image are in the same direction as in the original transmission line. Thus, the radiation contribution from the image transmission is expected to *add* to the original transmission line radiation. Thus, the radiation at node 3 from the line located near the ground plane is given by the expression

$$E_\xi = \frac{jk}{2\pi}\frac{Z_o}{Z_c}\left(\frac{e^{-jkr_o}}{r_o}+\frac{e^{-j(kr_o+2h)}}{(r_o+2h)}\right)\left(F_1(\psi_o)V_{1,1}^{inc}+F_2(\psi_o)V_{1,2}^{inc}\right)$$
$$\equiv \frac{jk}{2\pi}\frac{Z_o}{Z_c}K_1(r_o)\left(F_1(\psi_o)V_{1,1}^{inc}+F_2(\psi_o)V_{1,2}^{inc}\right) \quad , \qquad (21)$$

where the term K_1 is that defined in Eq.(14) and the angle $\psi_o = \pi/2$. Note that Eq.(21) assumes that the observation angles ψ_o from the physical and image transmission lines are equal, which is valid only for distant observation points.

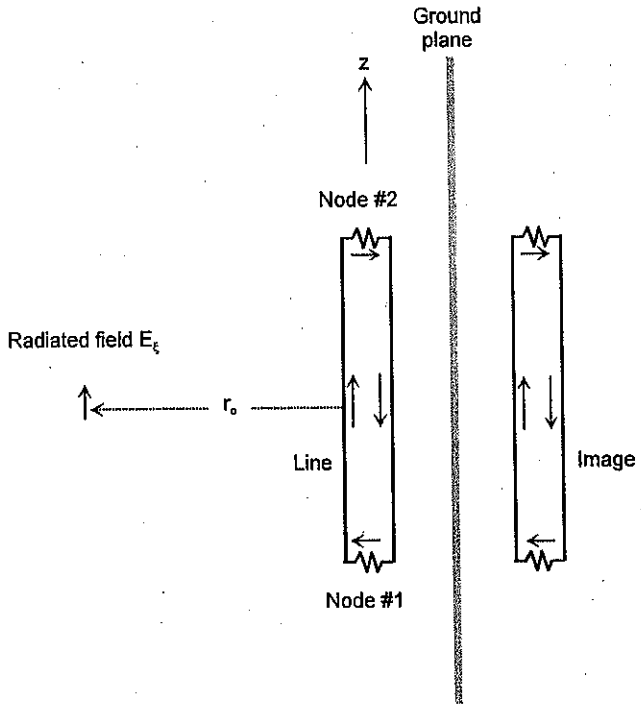

Figure 10. Radiation from the transmission line in the presence of the conducting ground.

With Eq.(21) providing the contribution from the transmission line currents to the incident field at node 3, we express the complete incident E-field at this node as

$$E_{2,3}^{inc} = K_2(r_o)a_4E_{2,4}^{ref} + K_3(r_2)\mathcal{S}_2(\psi_2) + \frac{jk}{2\pi}\frac{Z_o}{Z_c}K_1(r_o)\left(F_1(\psi_o)V_{1,1}^{inc} + F_2(\psi_o)V_{1,2}^{inc}\right) \quad (22)$$

Using the same procedure as in ref. [3], we combine Eqs.(18) and (22) into a matrix equation for the incident and reflected E-field components at nodes 3 and 4, as

$$\begin{bmatrix} E_{2,3}^{inc} \\ E_{2,4}^{inc} \end{bmatrix} = \begin{bmatrix} 0 & a_4K_2(r_o) \\ a_3K_2(r_o) & 0 \end{bmatrix} \cdot \begin{bmatrix} E_{2,3}^{ref} \\ E_{2,4}^{ref} \end{bmatrix} + \frac{jk}{2\pi}\frac{Z_o}{Z_c}K_1(r_o)\begin{bmatrix} F_1 & F_2 \\ 0 & 0 \end{bmatrix} \cdot \begin{bmatrix} V_{1,1}^{inc} \\ V_{1,2}^{inc} \end{bmatrix} + \begin{bmatrix} K_3(r_2)\mathcal{S}_2 \\ K_2(r_1)\mathcal{S}_1 \end{bmatrix} \quad (23)$$

and upon rearranging terms, this equation can be solved for the normalized *reflected* E-fields at the nodes as

$$\begin{bmatrix} a_3E_{2,3}^{ref} \\ a_4E_{2,4}^{ref} \end{bmatrix} = \begin{bmatrix} 0 & \frac{1}{a_4K_2(r_o)} \\ \frac{1}{a_3K_2(r_o)} & 0 \end{bmatrix} \begin{bmatrix} a_3E_{2,3}^{inc} \\ a_4E_{2,4}^{inc} \end{bmatrix} - \frac{jk}{2\pi}\frac{Z_o}{Z_c}\frac{K_1(r_o)}{K_2(r_o)}\begin{bmatrix} 0 & 0 \\ F_1 & F_2 \end{bmatrix} \begin{bmatrix} V_{1,1}^{inc} \\ V_{1,2}^{inc} \end{bmatrix} - \begin{bmatrix} \frac{K_2(r_1)}{K_2(r_o)}\mathcal{S}_1 \\ \frac{K_3(r_2)}{K_2(r_o)}\mathcal{S}_2 \end{bmatrix} \cdot$$

(24)

Equations (15) and (24) now can be combined into a larger matrix equation relating the reflected generalized voltage quantities at the nodes to the incident voltages and the source terms. See Appendix A of this report for details. The resulting equation is

$$\begin{bmatrix} V_{1,1}^{ref} \\ V_{1,2}^{ref} \\ a_3 E_{2,3}^{ref} \\ a_4 E_{2,4}^{ref} \end{bmatrix} = \begin{bmatrix} 0 & e^{\gamma L} & 0 & -\frac{K_1(r_o)}{a_4 K_2(r_o)} F_1 \\ e^{\gamma L} & 0 & 0 & -\frac{K_1(r_o)}{a_4 K_2(r_o)} F_2 \\ 0 & 0 & 0 & \frac{1}{a_4 K_2(r_o)} \\ -\frac{jk}{2\pi}\frac{Z_o}{Z_c}\frac{K_1(r_o)}{K_2(r_o)} F_1 & -\frac{jk}{2\pi}\frac{Z_o}{Z_c}\frac{K_1(r_o)}{K_2(r_o)} F_2 & \frac{1}{a_3 K_2(r_o)} & 0 \end{bmatrix} \begin{bmatrix} V_{1,1}^{inc} \\ V_{1,2}^{inc} \\ a_3 E_{2,3}^{inc} \\ a_4 E_{2,4}^{inc} \end{bmatrix} - \begin{bmatrix} F_1\left(\frac{K_1(r_1)K_2(r_0)-K_1(r_o)K_2(r_1)}{K_2(r_o)}\right) S_1 \\ F_2\left(\frac{K_1(r_1)K_2(r_0)-K_1(r_o)K_2(r_1)}{K_2(r_o)}\right) S_1 \\ \frac{K_2(r_1)}{K_2(r_o)} S_1 \\ \frac{K_3(r_2)}{K_2(r_o)} S_2 \end{bmatrix} \quad (25)$$

3.2 Node Reflection Relationships

At nodes 1 and 2 on the transmission line, the voltage reflection coefficients are used to related the reflected and incident voltage waves as

$$V_{1,1}^{ref} = \rho_1 V_{1,1}^{inc} \text{ and } V_{1,2}^{ref} = \rho_2 V_{1,2}^{inc} \quad (26a)$$

where the reflection coefficients ρ_i are related to the terminating line impedance and the line characteristic impedance as

$$\rho_i = \frac{Z_{Li} - Z_c}{Z_{Li} + Z_c}. \quad (26b)$$

Similarly, at node 3 we can define an E-field reflection coefficient between the field incident and reflected at this location – if there is a scattering body at this node. This relationship is

$$E_{2,3}^{ref} = \rho_3 E_{2,3}^{inc} . \quad (27)$$

If we assume that this observation point is located in free space, there is no reflection of the field, and we have the condition that $\rho_3 = 0$.

At node 4, the field coupling node, the effects of the transmission line currents in producing a reflected field at this node have already been taken into account in Eq.(22). However, the effects of the antenna mode current flowing on the transmission line have yet to be included in the analysis. As shown in Figure 11, the two wire line can be modeled as a single conductor of length L and effective radius $a_{eff} = \sqrt{2}\,a$, so that the equivalent cross-sectional area of the conductor is equal to the total area of the 2-wire line.

For this line, an incident EM-field with polarity as noted in the figure strikes the wire with an angle of incidence θ_i. This field induces a current $I(z)$ to flow in the wire and a

scattered EM field results in such a way that the total tangential E-field is zero along the wire. The is $\hat{\theta}$ component of the scattered E-field may at an observation angle θ_s is shown in the diagram.

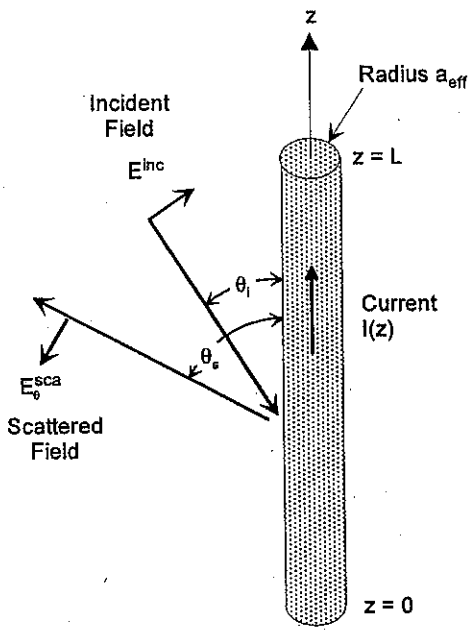

Figure 11. Illustration of a single conductor scatterer of length L and radius a_{eff}.

For use in the extended BLT equation, we need a relationship between the incident field at this wire to the scattered field to define the field reflection coefficient at node 4. The usual approach for determining this is to use an integral equation solution. However, keeping with the spirit of performing a transmission line analysis for this analysis, we can develop an approximate, transmission line-like analysis for this scattering problem.

As noted in Chapter 4 of ref.[2], the Hallén integral equation for the antenna mode current for the conductor in Figure 11 can be approximated and a closed-form of the incident field-induced current results. For an incident field E^{inc} at angle θ_i, this current has the form

$$I(z) = \frac{j4\pi E^{inc}}{Z_c \Omega_o k \sin\theta_i}\left[\left(\cos kz - e^{jkz\cos\theta_i}\right) + \left(e^{jkL\cos\theta_i} - \cos kL\right)\frac{\sin kz}{\sin kL}\right] . \qquad (28)$$

In this expression, the term Ω is the usual thin-wire antenna parameter, $\Omega = 2\ln(L/a)$.

The scattered E-field at the angle θ_s can be determined from integration over the wire current distribution as

$$E_\theta^{sca} = \frac{jkZ_c \sin\theta_o}{4\pi}\frac{e^{-jkr_o}}{r_o}\int_0^L I(z)\, e^{jkz\cos\theta_o} dz$$
$$= -\frac{E^{inc}}{\Omega_o}\frac{\sin\theta_o}{\sin\theta_i}\frac{1}{\sin(kL)}\frac{e^{-jkr_o}}{r_o}\int_0^L \left[\left(\cos kz - e^{jkz\cos\theta_i}\right)\sin kL - \left(\cos kL - e^{jkL\cos\theta_i}\right)\sin kz\right] e^{jkz\cos\theta_o} dz . \quad (29)$$

where $k = \omega/c$. As noted in [2], the analytical expression for the scattered field for arbitrary angles θ_i and θ_s are very cumbersome. However for $\theta_i = \theta_s = \pi/2$ the expression is rather simple:

$$E_\theta^{sca} = \frac{E^{inc}}{\Omega_o}\frac{e^{-jkr_o}}{kr_o}\frac{\left(2(\cos(kL)-1)+kL\sin(kL)\right)}{\sin(kL)} \quad (30)$$

For the reflection coefficient at node 4, we wish to relate the z-components of the fields. Noting that $E_\theta^{sca} = -E_z^{sca}$, we have from Eq.(30)

$$E_z^{sca} = \frac{E^{inc}}{\Omega_o}\frac{e^{-jkr_o}}{kr_o}\frac{\left(2(1-\cos(kL))-kL\sin(kL)\right)}{\sin(kL)}$$
$$= E^{inc}\frac{e^{-jkr_o}}{r_o}\sigma(\omega) \quad (31)$$

where $\sigma(\omega)$ is the frequency dependent *effective scattering length* of the wire, defined as

$$\sigma(\omega) \equiv \frac{c}{\Omega_o \omega L}\frac{\left(2(1-\cos(\omega L/c))-kL\sin(\omega L/c)\right)}{\sin(\omega L/c)} \text{ (meters)} . \quad (32a)$$

The above expression for the effective scattering length is seen to have zeros in the denominator due to the term $\sin(\omega L/c)$. Frequencies for which $(\omega L/c) = n\pi$ correspond to the natural resonant frequencies of the antenna mode current on the wire, and at these frequencies the scattering length given in Eq.(32a) is infinite. This singularity arises because the radiation loss of the scatterer is not properly taken into account in the approximate scattering analysis.

In a numerical implementation of the extended BLT equation, these singularities in σ provide similar singularities in the spectrum of the computed E-fields at the field nodes 3 and 4. Moreover, in the time domain, the FFT solution consists of an ever-repeating oscillating waveform with the frequency content of the various singularities.

To fix this problem, we can add artificial loss into the antenna mode solution – not trying to model accurately the radiation resistance, but rather, attempting to eliminate the singularities in the solution. Noting that the derivation of the antenna mode response has involved a transmission line-like equation, we can put Eq.(32a) into a form resembling a transmission line solution by expanding the $\sin(\omega L/c)$ term into complex exponentials. In this manner, Eq.(32a) can be written as

$$\sigma(\omega) = \frac{-2je^{j\omega L/c}}{\Omega_o \omega/c} \frac{\left(2(1-\cos(\omega L/c)) - (\omega L/c)\sin(\omega L/c)\right)}{e^{j2\omega L/c} - 1} \qquad (32b).$$

In examining typical transmission line solutions (see ref.[2]), we note that the denominator term in the Eq.(32b) frequently appears as $e^{jk2\omega L/c} - \rho_1\rho_2$, where ρ_1 and ρ_2 correspond to voltage reflection coefficients. When ρ_1 and $\rho_2 = \pm 1$ there are zeros in the denominator and singularities in the response. However, when there is loss on the transmission line, the product of these reflection coefficients is $|\rho_1\rho_2| < 1$, with the result that there are no response singularities. Thus, a simple solution to eliminate these singularities is to rewrite the denominator in Eq.(32b) as $e^{jk2\omega L/c} - \kappa$, where κ is a suitably chosen number close to, but less than, unity. A choice for this parameter for this study is $\kappa = 0.9$.

To determine the reflection coefficient at node 4, we evaluate Eq.(31) at the node "boundary", which is defined by the parameter a_4 that was introduced in Eq.(18). At a distance of a_4 from the node, the scattered E-field is expressed in terms of the incident field as

$$\begin{aligned} E_z^{sca} &= E^{inc} \frac{e^{-jka_4}}{a_4} \sigma(\omega) \\ &\approx E^{inc} \frac{\sigma(\omega)}{a_4} \\ &\equiv E^{inc} \rho_4(\omega) \end{aligned} \qquad (33)$$

Hence the reflection coefficient is $\rho_4 = \sigma/a_4$ at node 4.

Taking each of the reflected terms into account, we now can write the network reflection matrix as

$$\begin{bmatrix} V_{1,1}^{ref} \\ V_{1,2}^{ref} \\ E_{2,3}^{ref} \\ E_{2,4}^{ref} \end{bmatrix} = \begin{bmatrix} \rho_1 & 0 & 0 & 0 \\ 0 & \rho_2 & 0 & 0 \\ 0 & 0 & \rho_3 & 0 \\ 0 & 0 & 0 & \rho_4 \end{bmatrix} \cdot \begin{bmatrix} V_{1,1}^{inc} \\ V_{1,2}^{inc} \\ E_{2,3}^{inc} \\ E_{2,4}^{inc} \end{bmatrix} \qquad (34a)$$

or in terms of the normalized voltage variables,

$$\begin{bmatrix} V_{1,1}^{ref} \\ V_{1,2}^{ref} \\ a_3 E_{2,3}^{ref} \\ a_4 E_{2,4}^{ref} \end{bmatrix} = \begin{bmatrix} \rho_1 & 0 & 0 & 0 \\ 0 & \rho_2 & 0 & 0 \\ 0 & 0 & \rho_3 & 0 \\ 0 & 0 & 0 & \rho_4 \end{bmatrix} \cdot \begin{bmatrix} V_{1,1}^{inc} \\ V_{1,2}^{inc} \\ a_3 E_{2,3}^{inc} \\ a_4 E_{2,4}^{inc} \end{bmatrix} \qquad (34b)$$

3.3 *The Extended BLT Equations*

Eqs.(25) and (34b) can now be solved for the vector of incident waves at the nodes. This provides the following *extended* BLT equation for the incident voltages and E-fields at the nodes:

$$\begin{bmatrix} V_{1,1}^{inc} \\ V_{1,2}^{inc} \\ a_3 E_{2,3}^{inc} \\ a_4 E_{2,4}^{inc} \end{bmatrix} = \begin{bmatrix} -\rho_1 & e^{\gamma L} & 0 & -\frac{K_1(r_o)}{a_4 K_2(r_o)} F_1 \\ e^{\gamma L} & -\rho_2 & 0 & -\frac{K_1(r_o)}{a_4 K_2(r_o)} F_2 \\ 0 & 0 & -\rho_3 & \frac{1}{a_4 K_2(r_o)} \\ -\frac{jk}{2\pi}\frac{Z_o}{Z_c}\frac{K_1(r_o)}{K_2(r_o)} F_1 & -\frac{jk}{2\pi}\frac{Z_o}{Z_c}\frac{K_1(r_o)}{K_2(r_o)} F_2 & \frac{1}{a_3 K_2(r_o)} & -\rho_4 \end{bmatrix}^{-1} \begin{bmatrix} F_1\left(\frac{K_1(r_1)K_2(r_0)-K_1(r_o)K_2(r_1)}{K_2(r_o)}\right) S_1 \\ F_2\left(\frac{K_1(r_1)K_2(r_0)-K_1(r_o)K_2(r_1)}{K_2(r_o)}\right) S_1 \\ \frac{K_2(r_1)}{K_2(r_o)} S_1 \\ \frac{K_3(r_2)}{K_2(r_o)} S_2 \end{bmatrix} \quad (35)$$

Using Eq.(34b) again in the above expression to compute the *total* voltage and E-field, we can write the final expression for the extended BLT equation as :

$$\begin{bmatrix} V_{1,1} \\ V_{1,2}^{t} \\ a_3 E_{2,3} \\ a_4 E_{2,4} \end{bmatrix} = \begin{bmatrix} 1+\rho_1 & 0 & 0 & 0 \\ 0 & 1+\rho_2 & 0 & 0 \\ 0 & 0 & 1+\rho_3 & 0 \\ 0 & 0 & 0 & 1+\rho_4 \end{bmatrix} \times$$

$$\begin{bmatrix} -\rho_1 & e^{\gamma L} & 0 & -\frac{K_1(r_o)}{a_4 K_2(r_o)} F_1 \\ e^{\gamma L} & -\rho_2 & 0 & -\frac{K_1(r_o)}{a_4 K_2(r_o)} F_2 \\ 0 & 0 & -\rho_3 & \frac{1}{a_4 K_2(r_o)} \\ -\frac{jk}{2\pi}\frac{Z_o}{Z_c}\frac{K_1(r_o)}{K_2(r_o)} F_1 & -\frac{jk}{2\pi}\frac{Z_o}{Z_c}\frac{K_1(r_o)}{K_2(r_o)} F_2 & \frac{1}{a_3 K_2(r_o)} & -\rho_4 \end{bmatrix}^{-1} \begin{bmatrix} F_1\left(\frac{K_1(r_1)K_2(r_0)-K_1(r_o)K_2(r_1)}{K_2(r_o)}\right) S_1 \\ F_2\left(\frac{K_1(r_1)K_2(r_0)-K_1(r_o)K_2(r_1)}{K_2(r_o)}\right) S_1 \\ \frac{K_2(r_1)}{K_2(r_o)} S_1 \\ \frac{K_3(r_2)}{K_2(r_o)} S_2 \end{bmatrix} \quad (36)$$

Note that this equation now contains the effects of the both the transmission line mode and the antenna mode response of the two-wire line.

3.4 *Solution to the Extended BLT Equation*

For the case where there is no reflection at node 3 ($\rho_3 = 0$), it is possible to obtain a symbolic solution to Eq.(36) for the total voltages and fields at the nodes. After a bit of manipulation, we can express these solutions as

$$V_{1,1} = (1+\rho_1)\frac{e^{\gamma L}F_2 + \rho_2 F_1}{e^{2\gamma L} - \rho_1\rho_2} K_1(r_1)\mathcal{S}_1 \tag{37a}$$

$$V_{1,2} = (1+\rho_2)\frac{e^{\gamma L}F_1 + \rho_1 F_2}{e^{2\gamma L} - \rho_1\rho_2} K_1(r_1)\mathcal{S}_1 \tag{37b}$$

$$E_{2,3} = K_3(r_2)\mathcal{S}_2 + \sigma K_2(r_o)K_2(r_1)\mathcal{S}_1 + \frac{jk}{2\pi}\frac{Z_o}{Z_c}K_1(r_o)K_1(r_1)\left(\frac{2F_1F_2e^{\gamma L} + F_1^2\rho_2 + F_2^2\rho_1}{e^{2\gamma L} - \rho_1\rho_2}\right)\mathcal{S}_1 \tag{37c}$$

$$E_{2,4} = \left(1+\frac{\sigma}{a_4}\right)K_2(r_1)\mathcal{S}_1 \tag{37d}$$

The voltage solutions in Eqs.(37a) and (37b) have the form of the usual transmission line solutions for the load voltages due to an incident field excitation. Note that the reflection coefficients ρ_1 and ρ_2 provide oscillations on the line, and the Green's function $K_1(r_1)$ contains the time delay and $1/r$ fall-off for the propagation of the excitation from the source and its image in the ground plane.

Equation (37c) for the total E-field at the observation node 3 is seen to have three components. The first is a direct illumination by the source and its image. The second term arises from the antenna mode scattering from node 4, which has been accounted for by the node 4 reflection coefficient ρ_4. The last term in Eq.(37c) arises from the differential mode scattering from the line, and as such, it contains the influence of the transmission line reflections. It is important to note that in this expression for the E-field at node 3, the node dimension parameter a3 that was introduced for dimensional consistency in Eq.(10) is not present. Clearly the value of this parameter is not important.

The final equation (37d) represents the solution for the total E-field at the field coupling node 4. We see that the field expression at this point consists of an incident component from the source and its image (through the single $K_2(r_1)$ term) and another term arising from the scattering effects of the antenna current (the $(\sigma/a_4)K_2(r_1)$ term). Ideally, this total field should be zero, due to the boundary condition that the total E-field on the scattering body is zero. However, we note that this approximate solution for the scattering from this wire does not provide for a null field.

Furthermore, there have been no contributions to the field at this node by the transmission line currents in Eq.(23). Had these contributions been included, the matrix of F terms would have been full, with the traveling wave currents providing incident wave contributions to node 4. Thus, the solution for the total field at node 4 is not obtainable from these approximate transmission line and scattering solutions. However, it is known to be zero.

4. Numerical Verification

To check on the validity of this extended BLT solution, several numerical examples have been considered using the geometry of Figure 2. The following parameters have been chosen to define a baseline geometry for this comparison:

Line length $L = 1$ m
Wire separation $d = 1$ cm
Wire radius a = 1 mm
Characteristic impedance $Z_c = 120 \ln(d/a) = 276.3\ \Omega$
Load resistances $Z_L = Z_c/2 = 138.15\ \Omega$
Line – ground plane distance $h = 3$ m
Source – line distance $r_1 = 10$ m
Source—field point distance $r_2 = 10$ m
All angles equal: $\psi_1 = \psi_2 = \psi_o = \psi_s = \pi/2$.

4.1 Consideration of an Isolated Transmission Line

The first check for this solution involves examining an *isolated* transmission line. By adjusting the current excitation source of Eq.(12) so that the incident E-field on the line is $E^{inc} = 1$ V/m, we can compute the load currents ($I_L = V_L/Z_L$) at each transmission line load using the extended BLT solution for the voltages from Eq.(36). For this isolated transmission line, the line length and wire radius given above were used, but a wire separation of $d = 2$ cm was used. Thus, the characteristic impedance of the line was $Z_c = 359.49\ \Omega$ and the load resistances were $Z_L = 179.74\ \Omega$.

Treating this transmission line as an incident field excitation problem, we have developed an alternate transmission line model, as discussed in [2]. The NULINE computer program was used to compute the current in load #1 on the transmission line, and the normalized response $|I_L/E^{inc}|$ is plotted in Figure 12a, overlaid with the extended BLT solution. The two curves are identical, as expected, because they are both formulated under the assumptions of transmission line theory.

Figure 12b presents the results of calculating the load current on the same transmission line structure using an integral equation solution embodied in the Numerical Electromagnetics Code (NEC) [4]. Comparing the *a* and *b* parts of this figure, we note an excellent agreement between the transmission line solutions and the NEC solution for frequencies above 100 MHz. Below this frequency, the NEC results are in error, due to the well-known code instability for loop structures at low frequencies.

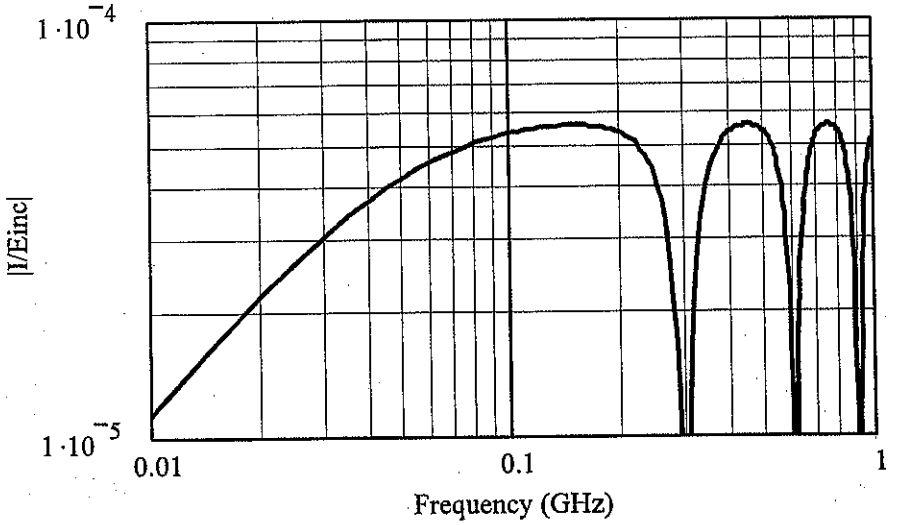

a. Overlay of the extended BLT and NULINE solutions.

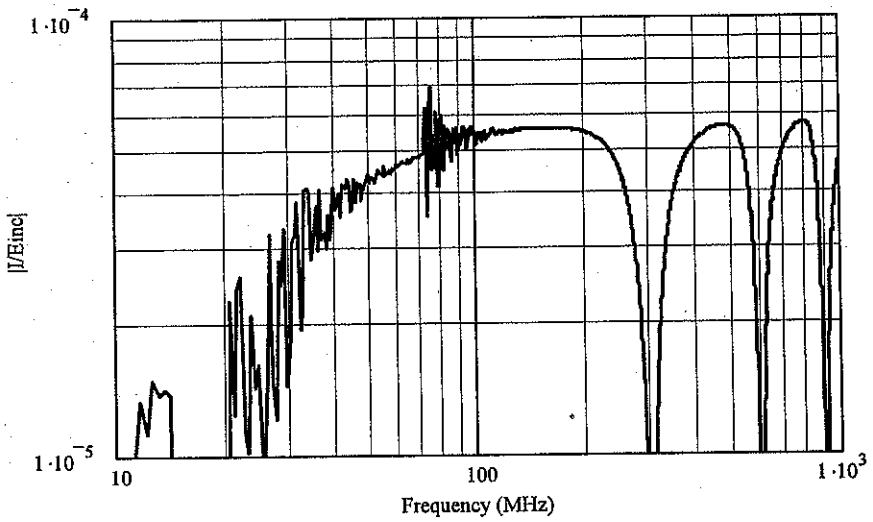

b. The NEC solution

Figure 12. Comparison of the extended BLT, NULINE and NEC solutions for the plane-wave-induced load current spectrum $|I_L/E^{inc}|$ for an isolated transmission line.

4.2 Transmission Line Voltages at Nodes 1 and 2

The above check of the isolated line case gives partial confidence in the validity of the extended BLT solution. However, for further examine the solution, we must include the ground plane in the problem. To show the computed results, we can examine the responses in the time domain where the times of arrival and polarity attributes of the response components can be easily seen. To this end, a simple unit amplitude double exponential waveform

$$i(t)\,dl = \left[\left(\frac{\alpha}{\beta}\right)^{\frac{\alpha}{\beta-\alpha}} - \left(\frac{\alpha}{\beta}\right)^{\frac{\beta}{\beta-\alpha}}\right]^{-1} \left(e^{-\alpha t} - e^{-\beta t}\right)\Phi(t) \qquad (38)$$

has been used to represent the time dependence of the current moment $i(t)\ dl$. For this waveform the following parameters are used:

$\alpha = 6.666 \times 10^7$ (1/s)
$\beta = 1.0 \times 10^9$ (1/s).

The term $\Phi(t)$ denotes the Heaviside function: $\Phi(t) = 0$ for $t \le 0$, $= 1$ for $t > 0$. Figure 13 displays this source excitation waveform and it spectral magnitude.

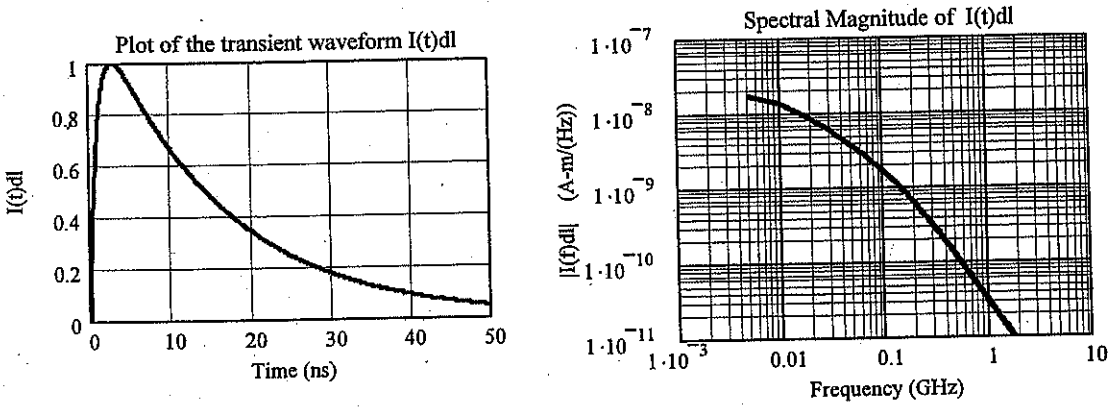

Figure 13. Plot of the transient behavior of the current moment $i(t)\ dl$ (left), and the corresponding spectral magnitude (right).

Calculating the load voltages from the extended BLT equation (36) for a unit excitation for the infinitesimal current element spectrum ($I(f)\ dl = 1$) yields the voltage response transfer function shown in Figure 14. Part *a* of the figure presents the transfer function magnitude for both of the load voltages (they are identical in magnitude) as determined by the BLT equation, and part *b* shows the corresponding responses for an integral equation solution – this time not using NEC, but rather, another integral equation solution developed by one of the authors (JK) for this comparison. As noted in this figure, the BLT transmission line model and the integral equation model yield virtually identical spectral results.

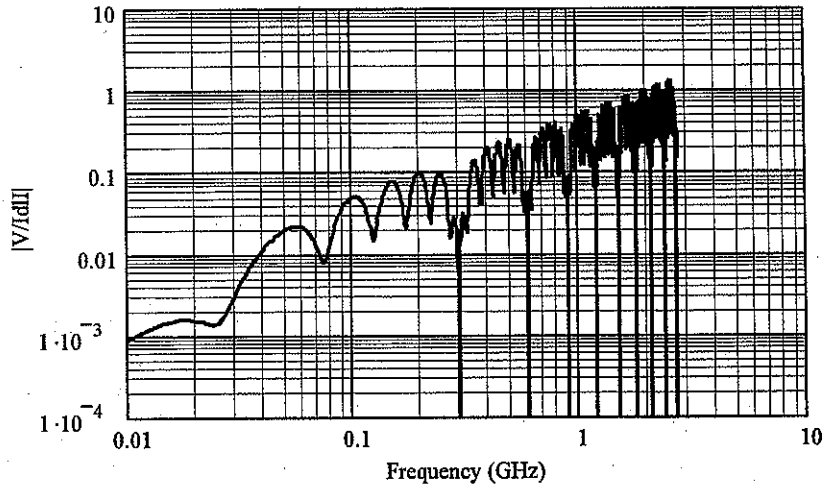

a. Extended BLT solution

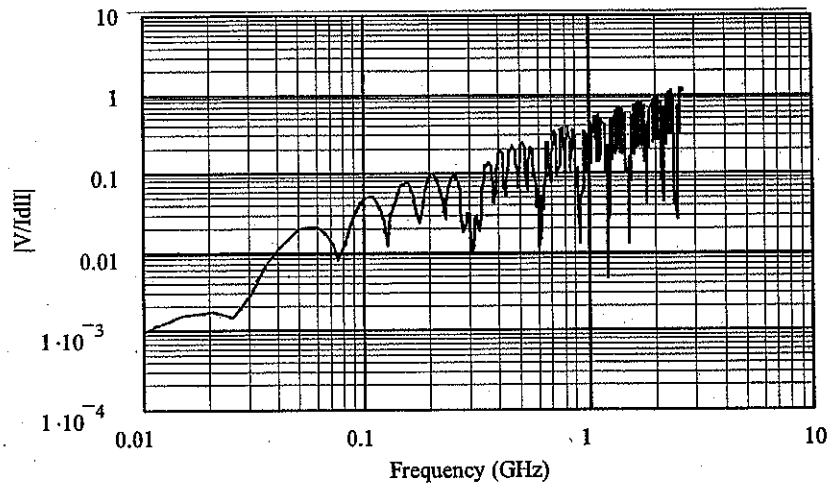

b. Integral equation solution

Figure 14. Plots of the extended BLT equation solution (*a*) and an integral equation solution (*b*) for the load voltage transfer function spectra $|V_L(f)/I(f)\ dl|$ for the transmission line shown in Figure 2 (baseline configuration).

The transient responses of the load voltages at nodes 1 and 2 of the transmission line is found by multiplying the transfer functions of Figure 14 by the excitation spectrum of Figure 13b and taking an inverse FFT[3]. These results are shown in Figure 15, with excellent agreement between the two methods being noted.

4.3 E-fields at the Observation Node

In addition to the two transmission line load voltages, the extended BLT equation provides the E-fields at the observation nodes 3 and 4. As noted earlier, the BLT equation solution at node is not valid, because it is located in the near-field of the transmission line. Transmission line theory is incapable of providing reliable information for the near fields.

However, the solution at node 3 is accurate. At this node the BLT solution contains the effects of the direct radiation from the pulsed current source, the radiation of the antenna mode current from the line, and the radiation effects of the transmission line current (each having the ground plane image effects included). This partitioning of the responses into three components has been noted in Eq.(37c).

For the baseline problem configuration, Figure 16a presents the complete E-field at node 3. The first response that is observed occurs at a time $t = 10/c = 33.333$ ns, and is due to the incident wave propagating 10 m from the pulsed current source. The second pulse occurs at a time $t = (10+(2x3)+20)/c = 120$ ns, and is the reflection of the incident field from the source in the ground plane. Of course, this waveform also contains the contributions from the antenna and transmission line mode currents, but these latter components are much smaller than the direct incident field component.

To illustrate the contributions from the antenna and transmission line currents, we temporarily set the parameters K_3, F_1 and F_2 to zero in the BLT equation. This suppresses the incident field. (See Eq.(37c for the role that these parameters play in the solution.) This results in the E-field waveform of Figure 16b, which contains only the antenna mode contributions. Note that this response is about a factor of 250 smaller than the complete solution – indicating that the scattered field from the line is not too important in determining the total field.

Similarly, by setting the parameters K_3 and σ to zero, we are able to compute the field response for just the transmission line currents. This response component is shown in Figure 16c, and is a factor of 3,500 smaller than the incident field response. Clearly, this transmission line component is unimportant in the total field solution.

---

[3] Note that the choice of the excitation waveform in this example is unfortunate, in that the waveform has a discontinuous derivative at t = 0. As noted in Eq.(12), the radiated E-field from the source is proportional to jω times the excitation spectrum, and the excitation function of the line in Eq.(13) has another term involving jω from the sums of the two exponential terms. These two factors of jω multiplying the excitation waveform spectrum amount to taking a second time derivative of the waveform, which, for the double exponential function, provides a delta-function contribution when the waveform turns on. These impulse function contributions are clearly evident in Figure 15.

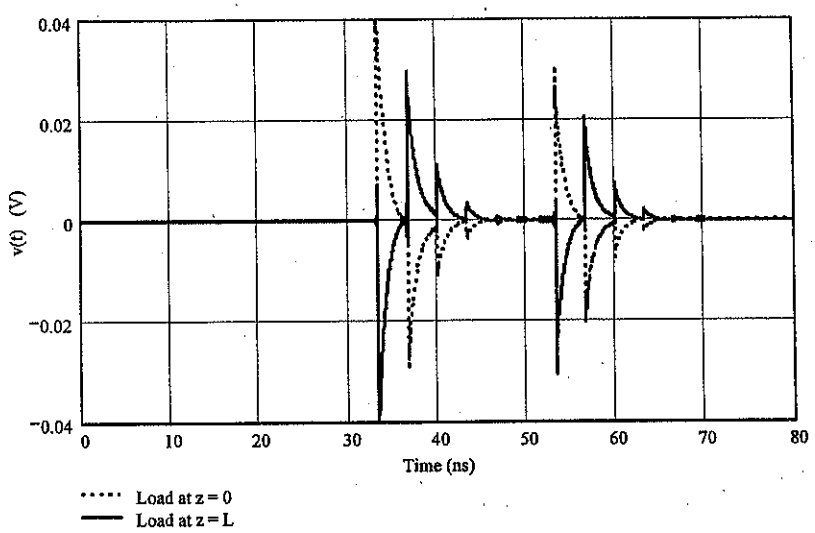

a. Extended BLT solution

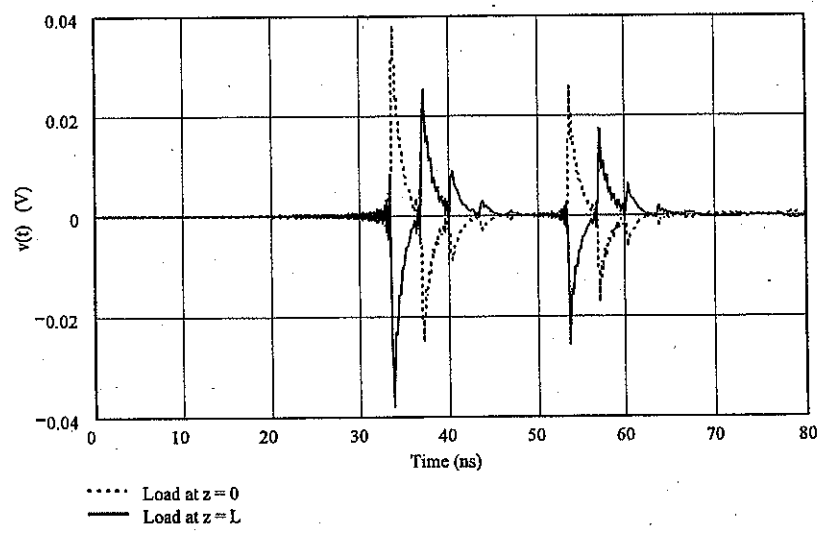

b. Integral equation solution

Figure 15. Plots of the transient BLT solution (*a*) and an integral equation solution (*b*) for the transient load voltages at both ends of the transmission line of Figure 2 (baseline configuration).

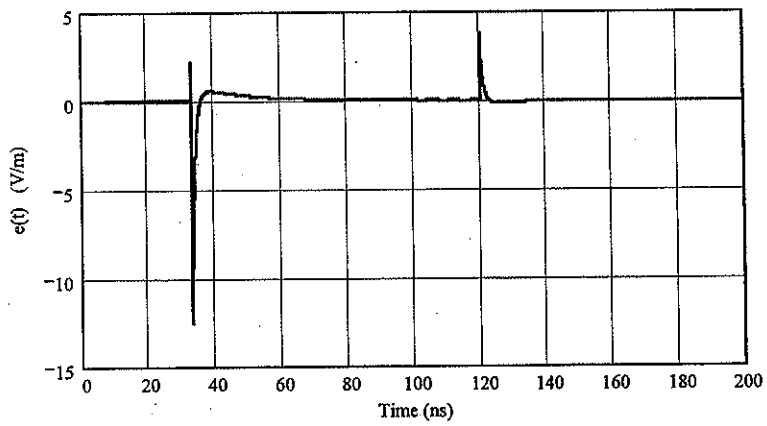

a. The radiated E-field at node 3

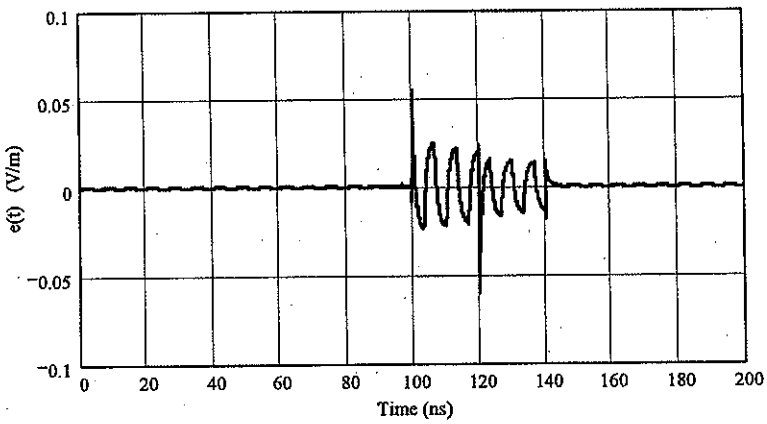

b. Radiated E-field at node 3 from only the antenna mode current.

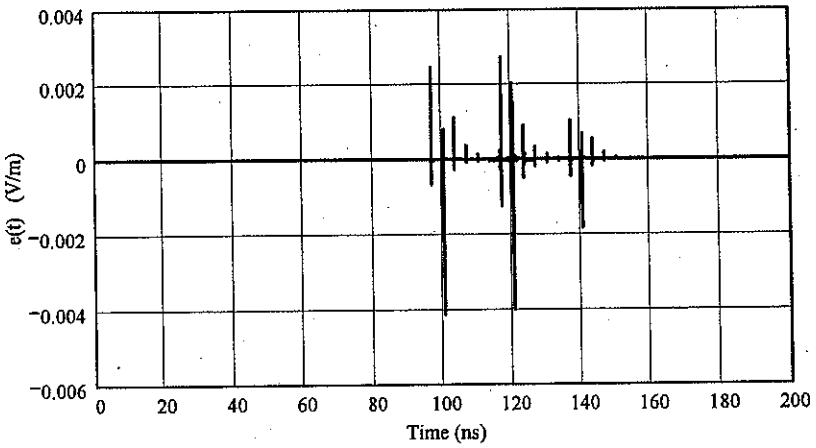

c. Radiated E-field at node 3 from only the transmission line currents.

Figure 16. Illustration of the radiated E-field at node 3. Part (*a*) is the total solution, (*b*) is the solution with just the antenna mode contribution, and (*c*) is only the transmission line contribution to the field.

5. Comments

This report has illustrated the development and use of the extended BLT equation for analyzing a transmission line located near a conducting ground plane and illuminated by an EM field produced by a near-by point source emitting a spherical wave. The extended BLT equation includes the transmission line voltage responses as observables, as well as the E-fields at observation nodes.

The solution of the transmission line responses uses conventional transmission line theory, with excitation being provided by the incident EM field from the source radiating in the presence of the ground plane. The ground plane effect on the solution is taken into account through modified Green's functions.

The solution for the radiating field components likewise uses modified Green's functions for the ground plane effect on the primary radiation from the point source. In addition, the radiation from the antenna mode and transmission line mode currents contribute to the E-fields at the observation locations.

All of these effects are combined together into an extended BLT equation, and this equation can be solved either numerically or symbolically. The numerical results that have been shown here are both reasonable and they have been verified partially by an independent integral equation analysis.

From the BLT analysis, it is clear that the E-field response computed at the transmission line is incorrect because the transmission line theory fails to provide accurate near-field results on the line. However, the transmission line load responses and the distant scattered field are accurate – within the limits afforded by the transmission line approximation. As noted in the comparison of the "exact" and approximate transmission line solutions, the agreement is very good.

There are several suggestions as to possible future work in this area of BLT analysts. These are as follows:

1. Examine the use of the modified Green's function approach to consider a transmission line located within a rectangular cavity, for example, where the Green's function can be expressed analytically.

2. Develop an analysis for the EM field coupling through an aperture in the ground plane (shield) that couples to a transmission line located on the opposite side of the shield.

3. Extend the BLT formalism to be able to represent a general EM radiation and scattering problem, taking into account all aspects of EM coupling (e.g., integral equation analysis), angle of incidence and polarization issues.

6. References

1. Baum, C.E., Liu, T.K, & Tesche, F.M., "On the Analysis of General Multiconductor Transmission Line Networks", *Interaction Note 350*, Kirtland AFB, NM, 1978.

2. Tesche, F. M., et. al., **EMC Analysis Methods and Computational Models**, John Wiley and Sons, New York, 1997.

3. Tesche, F. M., and C. M. Butler, "On the Addition of EM Field Propagation and Coupling Effects in the BLT Equation", *Interaction Notes*, Note 558, December 13, 2003.

4. Burke, G. J., and A. J. Poggio, "Numerical Electromagnetic Code (NEC) - Method of Moments," NOSC Tech. Doc. 116, Naval Ocean Systems Center, San Diego, CA, January 1980.

Appendix A

Combination of the Transmission Line and Field Propagation Relations for the Extended BLT Equation

Equations (15) and (24) provide the propagation relationships between the incident and reflected voltage waves on the transmission line and the field propagation path, as

$$\begin{bmatrix} V_{1,1}^{ref} \\ V_{1,2}^{ref} \end{bmatrix} = \begin{bmatrix} 0 & e^{\gamma L} \\ e^{\gamma L} & 0 \end{bmatrix} \cdot \begin{bmatrix} V_{1,1}^{inc} \\ V_{1,2}^{inc} \end{bmatrix} - \begin{bmatrix} F_1 K_1(r_o) a_3 E_{2,3}^{ref} \\ F_2 K_1(r_o) a_3 E_{2,3}^{ref} \end{bmatrix} - \begin{bmatrix} F_1 K_1(r_1) \mathcal{S}_1 \\ F_2 K_1(r_1) \mathcal{S}_1 \end{bmatrix} \tag{15}$$

$$\begin{bmatrix} a_3 E_{2,3}^{ref} \\ a_4 E_{2,4}^{ref} \end{bmatrix} = \begin{bmatrix} 0 & \frac{1}{a_4 K_2(r_o)} \\ \frac{1}{a_3 K_2(r_o)} & 0 \end{bmatrix} \begin{bmatrix} a_3 E_{2,3}^{inc} \\ a_4 E_{2,4}^{inc} \end{bmatrix} - \frac{jk}{2\pi} \frac{Z_o}{Z_c} \frac{K_1(r_o)}{K_2(r_o)} \begin{bmatrix} 0 & 0 \\ F_1 & F_2 \end{bmatrix} \begin{bmatrix} V_{1,1}^{inc} \\ V_{1,2}^{inc} \end{bmatrix} - \begin{bmatrix} \frac{K_2(r_1)}{K_2(r_o)} \mathcal{S}_1 \\ \frac{K_3(r_2)}{K_2(r_o)} \mathcal{S}_2 \end{bmatrix} \tag{24}$$

We would like to combine these into a single 4 x 4 matrix equation, but unfortunately, Eq.(15) has reflected wave components on the right hand side of the equation as well as on the left side. Thus a bit of matrix manipulation is required to arrive at the final matrix equation.

As may be easily verified, Eqs.(15) and (24) can be written together as

$$\begin{pmatrix} 1 & 0 & F_1 K_1(r_o) & 0 \\ 0 & 1 & F_2 K_1(r_o) & 0 \\ 0 & 0 & 1 & 0 \\ 0 & 0 & 0 & 1 \end{pmatrix} \begin{pmatrix} V_{1,1}^{ref} \\ V_{1,2}^{ref} \\ a_3 E_{2,3}^{ref} \\ a_4 E_{2,4}^{ref} \end{pmatrix} = \begin{pmatrix} 0 & e^{\gamma L} & 0 & 0 \\ e^{\gamma L} & 0 & 0 & 0 \\ 0 & 0 & 0 & \frac{1}{a_4 K_2(r_o)} \\ \frac{-jk}{2\pi} \frac{Z_o}{Z_c} \frac{K_1(r_o)}{K_2(r_o)} F_1 & \frac{-jk}{2\pi} \frac{Z_o}{Z_c} \frac{K_1(r_o)}{K_2(r_o)} F_2 & \frac{1}{a_3 K_2(r_o)} & 0 \end{pmatrix} \begin{pmatrix} V_{1,1}^{inc} \\ V_{1,2}^{inc} \\ a_3 E_{2,3}^{inc} \\ a_4 E_{2,4}^{inc} \end{pmatrix} - \begin{pmatrix} 0 & 0 & F_1 K_1(r_1) & 0 \\ 0 & 0 & F_2 K_1(r_1) & 0 \\ 0 & 0 & \frac{K_2(r_1)}{K_2(r_o)} & 0 \\ 0 & 0 & 0 & \frac{K_3(r_2)}{K_2(r_o)} \end{pmatrix} \begin{pmatrix} 0 \\ 0 \\ \mathcal{S}_1 \\ \mathcal{S}_2 \end{pmatrix} \tag{A1}$$

Noting that

$$\begin{pmatrix} 1 & 0 & F_1 K_1(r_o) & 0 \\ 0 & 1 & F_2 K_1(r_o) & 0 \\ 0 & 0 & 1 & 0 \\ 0 & 0 & 0 & 1 \end{pmatrix}^{-1} = \begin{pmatrix} 1 & 0 & -F_1 K_1(r_o) & 0 \\ 0 & 1 & -F_2 K_1(r_o) & 0 \\ 0 & 0 & 1 & 0 \\ 0 & 0 & 0 & 1 \end{pmatrix}, \tag{A2}$$

Eq.(A1) becomes

$$\begin{pmatrix} V_{1,1}^{ref} \\ V_{1,2}^{ref} \\ a_3 E_{2,3}^{ref} \\ a_4 E_{2,4}^{ref} \end{pmatrix} = \begin{pmatrix} 1 & 0 & -F_1 K_1(r_o) & 0 \\ 0 & 1 & -F_2 K_1(r_o) & 0 \\ 0 & 0 & 1 & 0 \\ 0 & 0 & 0 & 1 \end{pmatrix} \left[\begin{pmatrix} 0 & e^{\gamma L} & 0 & 0 \\ e^{\gamma L} & 0 & 0 & 0 \\ 0 & 0 & 0 & \frac{1}{a_4 K_2(r_o)} \\ \frac{-jk}{2\pi}\frac{Z_o}{Z_c}\frac{K_1(r_o)}{K_2(r_o)}F_1 & \frac{-jk}{2\pi}\frac{Z_o}{Z_c}\frac{K_1(r_o)}{K_2(r_o)}F_2 & \frac{1}{a_3 K_2(r_o)} & 0 \end{pmatrix} \begin{pmatrix} V_{1,1}^{inc} \\ V_{1,2}^{inc} \\ a_3 E_{2,3}^{inc} \\ a_4 E_{2,4}^{inc} \end{pmatrix} - \begin{pmatrix} 0 & 0 & F_1 K_1(r_1) & 0 \\ 0 & 0 & F_2 K_1(r_1) & 0 \\ 0 & 0 & \frac{K_2(r_1)}{K_2(r_o)} & 0 \\ 0 & 0 & 0 & \frac{K_3(r_2)}{K_2(r_o)} \end{pmatrix} \begin{pmatrix} 0 \\ 0 \\ S_1 \\ S_2 \end{pmatrix} \right] \quad \text{(A3)}$$

Carrying out the indicated matrix multiplications yields the final propagation matrix equation, which is Eq.(25):

$$\begin{pmatrix} V_{1,1}^{ref} \\ V_{1,2}^{ref} \\ a_3 E_{2,3}^{ref} \\ a_4 E_{2,4}^{ref} \end{pmatrix} = \begin{bmatrix} 0 & e^{\gamma L} & 0 & -\frac{K_1(r_o)}{a_4 K_2(r_o)}F_1 \\ e^{\gamma L} & 0 & 0 & -\frac{K_1(r_o)}{a_4 K_2(r_o)}F_2 \\ 0 & 0 & 0 & \frac{1}{a_4 K_2(r_o)} \\ -\frac{jk}{2\pi}\frac{Z_o}{Z_c}\frac{K_1(r_o)}{K_2(r_o)}F_1 & -\frac{jk}{2\pi}\frac{Z_o}{Z_c}\frac{K_1(r_o)}{K_2(r_o)}F_2 & \frac{1}{a_3 K_2(r_o)} & 0 \end{bmatrix} \cdot \begin{pmatrix} V_{1,1}^{inc} \\ V_{1,2}^{inc} \\ a_3 E_{2,3}^{inc} \\ a_4 E_{2,4}^{inc} \end{pmatrix} - \begin{bmatrix} F_1\left(\frac{K_1(r_1)K_2(r_0)-K_1(r_o)K_2(r_1)}{K_2(r_o)}\right)S_1 \\ F_2\left(\frac{K_1(r_1)K_2(r_0)-K_1(r_o)K_2(r_1)}{K_2(r_o)}\right)S_1 \\ \frac{K_2(r_1)}{K_2(r_o)}S_1 \\ \frac{K_3(r_2)}{K_2(r_o)}S_2 \end{bmatrix} \quad \text{(A4)}$$